Shear and AC Field Enhanced Carbon Nanotube Impedance Assay for Rapid, Sensitive, and Mismatch-Discriminating DNA Hybridization

Sagnik Basuray,[†] Satyajyoti Senapati,[†] Andrew Aijian,[†] Andrew R. Mahon,[‡] and Hsueh-Chia Chang[†,*]

[†]Department of Chemical and Biomolecular Engineering and [‡]Center for Aquatic Conservation, Department of Biological Sciences, University of Notre Dame, Indiana 46556

Rapid and highly sensitive RNA/DNA hybridization assays have attracted enormous attention in a wide variety of applications ranging from genotyping to molecular diagnosis.[1,2] Conventional lab-based optical detection methods for hybridization assays, such as microarray and real-time PCR, involve expensive detection protocols based on fluorescent tagging, thus requiring qualified professionals and limiting their potential use. Furthermore, DNA hybridization reactions in microarray analyses are time-consuming due to rate-limiting diffusion kinetics, making the technique difficult for point-of-need and high-throughput applications.[3−5] Thus, there is a need to develop label-free and rapid DNA/RNA hybridization platforms for applications ranging from genomics sequencing to pathogen identification.

This desired hybridization technology is consistent with modern diagnostic market demands for extremely sensitive, yet inexpensive, simple, rapid, and robust detection platforms that do not involve extensive sample pretreatments. Recent advances in electrochemical sensing techniques, in conjunction with nanotechnology and microfluidics, have shown great promise, offering more viable solutions than current optical sensing techniques.[6,7] The utilization of carbon nanotube (CNT) technology in these electrochemical sensors is particularly encouraging. Large surface area, flexible surface chemistry, wide electrochemical window, biocompatibility, and fast electron transfer kinetics for a wide range of electroactive species make carbon nanotubes a promising nanomaterial for electrochemical molecular recognition.[8] Furthermore,

ABSTRACT Other than concentrating the target molecules at the sensor location, we demonstrate two distinct new advantages of an open-flow impedance-sensing platform for DNA hybridization on carbon nanotube (CNT) surface in the presence of a high-frequency AC electric field. The shear-enhanced DNA and ion transport rate to the CNT surface decouples the parasitic double-layer AC impedance signal from the charge-transfer signal due to DNA hybridization. The flow field at high AC frequency also amplifies the charge-transfer rate across the hybridized CNT and provides shear-enhanced discrimination between DNA from targeted species and a closely related congeneric species with three nucleotide mismatches out of 26 bases in a targeted attachment region. This allows sensitive detection of hybridization events in less than 20 min with picomolar target DNA concentrations in a label-free CNT-based microfluidic detection platform.

KEYWORDS: bioassay · carbon nanotube · DNA hybridization · impedance · open flow

conventional capacitance electrochemical sensing techniques, such as those involving probes anchored onto thiol or other self-assembled monolayers on gold electrodes, rely on capacitance change after hybridization and are sensitive to buffer ionic strength and its effect on the double-layer capacitance.[9−11] In contrast, direct DNA absorption and hybridization onto CNTs can significantly enhance the electron-transfer rate, even if the molecular probes are relatively long and the hybridized target molecules are several nanometers away from the CNT. Without the poorly conducting monolayer, the DC conductance or AC reactance is much higher and hence the resistance sensing CNT platform has much higher signal/noise ratio than conventional capacitance sensing.[8]

Previous studies have successfully demonstrated the integration of individually addressable CNT microelectrode arrays, coupled with microelectronics and microfluidic systems, in bioassays to exemplify advantages of miniaturization and

multiplex detection.[9−16] Recent studies suggest that the use of electrokinetics, driven by electric fields sustained by embedded electrodes in microfluidic chips, precisely regulate the transport, concentration, and hybridization of oligonucleotides.[13] Zhou *et al.* reported the capture, concentration, and detection of bacteria through adsorption on CNT surface using dielectrophoresis, an AC electrokinetic technique.[14] More recently, Li *et al.* reported an ultrasensitive chemical and DNA detection technique by integrating a CNT-based electrode to an electrochemical system.[15] They found that the sensitivity of detection can be further improved by doping the system with an external redox species, $Ru(bpy)_3^{2+}$, which helps to promote electron-transfer rate by mediating guanine oxidation.[15] Detection of real-time DNA hybridization using CNT field-effect transistors (CNTFET) has been demonstrated by amino-modified peptide nucleic acid functionalized on gold surface of the back gate.[16] The detection is achieved by measuring the electrical characteristics of CNTFETs as the conductance of CNT changes because of DNA docking on the surface.[16] Xu *et al.* reported electrochemical impedance-based DNA biosensors using polymerized polypyrrole onto glassy carbon electrode and multiwall carbon nanotube.[17]

However, previous electrochemical CNT detection platforms involve passive hybridization protocol in a batch process and are relatively slow (∼hours) due to inherent diffusion-limited reaction kinetics. Another drawback of surface assay platforms is the limited specific binding sites for hybridization of DNA. Furthermore, in batch processes, the double-layer capacitor near the electrode surface masks the charge-transfer reaction kinetics on the electrode surface. This complicates the quantitative interpretation of experimental results.[18] An inexpensive CNT conductivity/impedance sensor platform that allows for sensitive, specific, and rapid detection of DNA hybridization is warranted.

To realize these stringent specifications for a viable DNA CNT hybridization platform, we report herein an open-flow-based simple, rapid, inexpensive, specific, and label-free microfluidic DNA hybridization detection platform. A solution containing the target single-stranded DNA polymerase chain reaction product (ssPCR) is passed through CNTs trapped by dielectrophoresis by an AC electric field supplied by two interdigited electrodes in a microchannel and is detected by the observed change in impedance due to docking of target DNA to the oligo probe functionalized on the CNT surface. The strong dielectrophoretic force on the CNTs[14] can hold them against a strong flow, thus eliminating the need for growing them on the electrodes or housing them in a microfilter trap whose high hydrodynamic resistance disallows high throughput. The detection is rapid and requires approximately 20 min from the time of passage of DNA through the CNT trap. The platform is highly specific and can distinguish between three mismatched bases within the targeted region of the target organism and a closely related, congeneric species. This is attributed to large hydrodynamic shear force ($>10^4$ s^{-1}) that can cleave or alter the conformation of any nonspecific binding of congener DNA to the probe or to the CNT surface in the presence of a high-frequency AC field. This open-flow rapid electrochemical microfluidic detection platform for DNA hybridization demonstrates the discrimination of a minimum of three mismatched DNA bases by hydrodynamic shear force. The platform also enhances detection sensitivity by allowing the passage of a large sample volume of low target DNA concentration. The flow helps to concentrate the target DNA molecules in the CNT trapping region, thus improving detection sensitivity to picomolar detection levels, as well as reducing the diffusion length to the separation between the CNTs. The detection time is then determined not by diffusion but by how fast the flow can transport sufficient target DNAs to the CNT sensor to produce a detectable signal. Another advantage of open-flow platform is that it minimizes the masking of the impedance signal by electrical double layer on electrode surface, which otherwise intervenes in batch processes and hence enhances the electron-transfer signal due to hybridization.

RESULTS AND DISCUSSION

Figure 1 depicts the schematic representation of open-flow CNT-based DNA hybridization platform with the channel inset to show different zones and the electrode arrangements. In electrochemical studies of biomolecules by impedance measurements, the electronic and ionic currents around the electrode surface are governed by the Randle circuit (Figure 2).[19−22] Randle circuit includes bulk solution resistance, R_S, double-layer capacitance, C_{dl}, at the electrode surface because of ions in the solution, a charge-transfer resistance or polarization resistance, R_{Ct}, that represents current flow due to redox reactions at the electrode−fluid interface and a constant phase element, the Warburg impedance signal. With a real part that is equal to its imaginary part, the Warburg impedance has a distinct impedance signature that is a linear locus in the complex plane with a 45° angle, as sketched out in the low-frequency limit in Figure 2. This Warburg impedance signature captures the diffusion of ions participating in the electron-transfer redox reaction toward the CNT electrode.[19−22] Hybridization is assumed to affect the electron-transfer rate, R_{Ct}, which is the desired quantity to be obtained from the real part of the impedance spectrum (conventional electrochemical sensing relies on the imaginary capacitance component). This value corresponds to the high-frequency limit of the linear Warburg branch in Figure 2, where it intersects the real axis. Unfortunately, this high-frequency intercept is of-
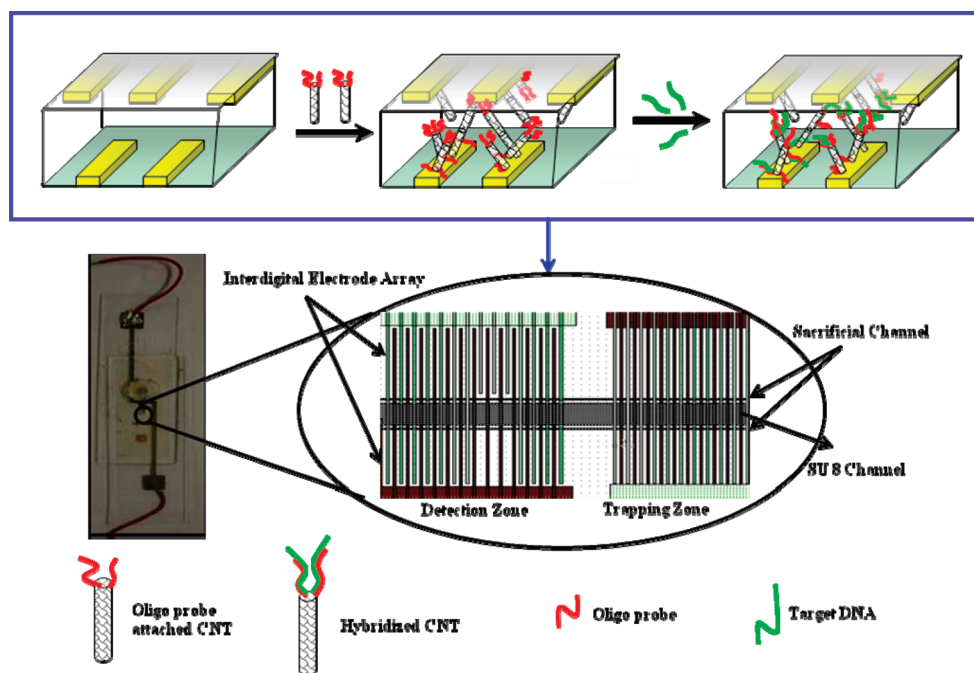
Figure 1. Schematic diagram of the chip is shown with the channel (inset) blown up to show the different zones and the interdigitated electrodes with the sacrificial channel. The hybridization protocol is shown as a representative cartoon.

ten camouflaged by the circular double-layer imped-ance loop that appears also at high frequencies (Figure 2). The double-layer capacitance, C_{dl}, which is inversely proportional to the Debye layer thickness, and the bulk resistance, R_S, typically produces an RC time of 10 μs and hence introduces the circular Debye branch when the frequency exceeds 100 kHz, which is below the high-frequency limit of the linear Warburg branch. As such, the Warburg and Debye branches overlap (Figure 2), and the precise estimate of R_{Ct} must be obtained with a careful analysis of the intersecting regions with sensitive impedance studies.[19−22]

Previous batch impedance studies with CNT electrodes for detection of DNA hybridization show the intersection of the Warburg branch with the double-layer branch.[17,23−28] However, the two branches decouple when a sufficient number of hybridized DNA form a film on the CNT electrode[24] and shift the intercept of the Warburg branch toward lower frequencies.[17,24,25] However, film formation only occurs at high DNA concentrations and hence reduces the sensitivity of the sensor.[17,25] To magnify the sensitivity, macro-ions such as Ru(biPyr)$^{2+}$/Daumoycin have been used to increase the electronic current and change R_{Ct}.[17,26,27] In contrast, with our flow effect, the mass transfer rate to the bulk is increased, which decreases R_S and the RC time for double-layer capacitor. This shifts the double-layer loop (Figure 2) to higher frequencies (Figure 3A). Without the double-layer loop, which masks the Warburg branch, impedance resolution of the electron-transfer rate significantly enhances the sensitivity of the sensor without the aid of macro-ions. The sensing platform is

also expected to be more robust to buffer ionic strength variations, which affects the double-layer RC time.

To understand the effect of flow on the double-layer branch, a series of experiments are designed to observe the changes in the impedance pattern with the sequential removal of double-layer branch by flow using three different chips. Mostly unsealed, partially sealed, and completely sealed chips are fabricated, and DNA experiments are performed by trapping the CNT within the channel and by passing the target DNA solution through it in the presence of an AC field. As the
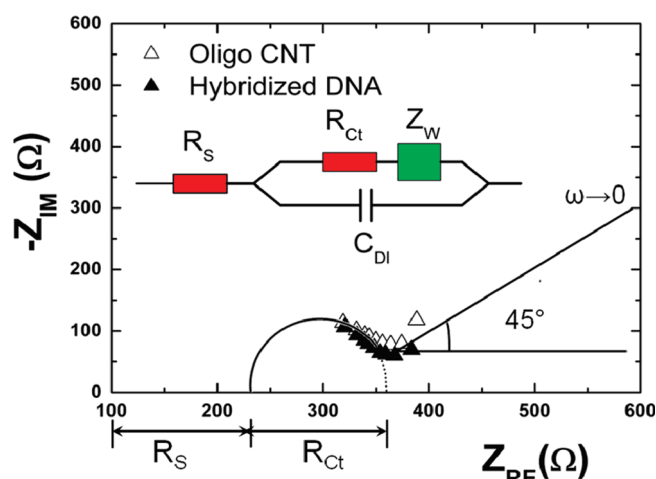

Figure 2. Graphical presentation of the Nyquist diagram for a Randle circuit with an inset of schematic diagram of the circuit is shown. Typical batch Nyquist plots are shown for hybridized and unhybridized oligo-CNTs in 4× SSC buffer solution in an applied AC field of 1 V at a frequency of 1 MHz. Extrapolation to obtain R_{Ct} is not possible due to the loop double-layer impedance signature. In fact, both hybridized and unhybridized data are indistinguishable at the important high-frequency end of the Warburg branch.
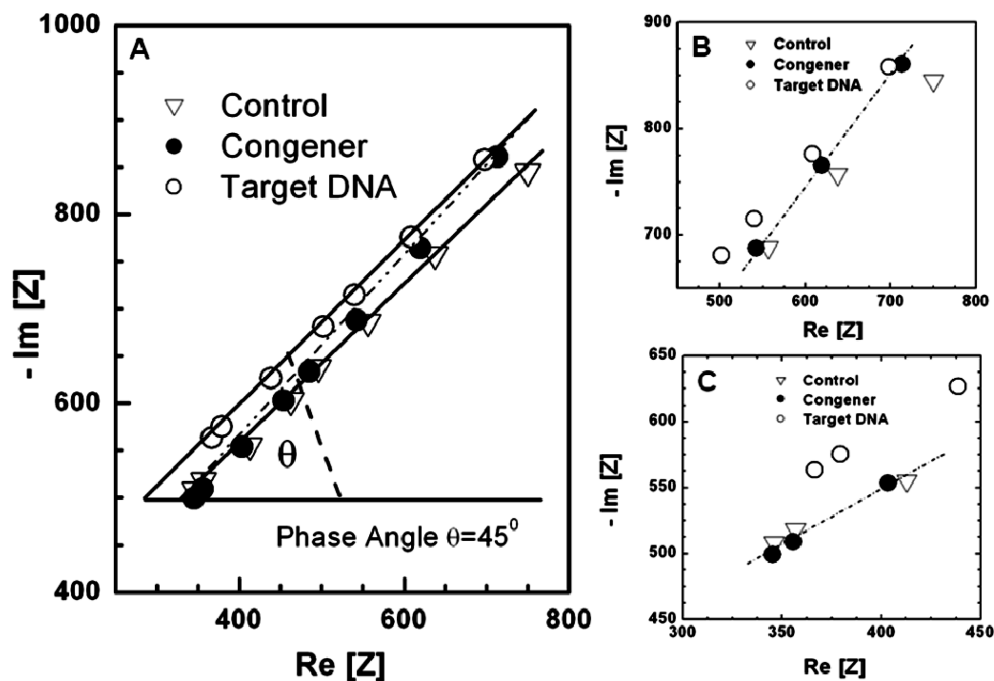
Figure 3. (A) Open-flow Nyquist impedance plots for the control, congener, and target DNA sample in PBS buffers are shown. The solutions are passed through the chip at a flow rate of 0.2 mL/h with the AC field activated at the interdigitated electrodes. The plot shows the Warburg impedance as a straight line at higher frequencies. The dashed line shows the asymptotic behavior of the congener at low and high frequencies. Panel A is divided into two figures to amplify the asymptotic behavior of the congener DNA at low (B) and high (C) frequencies.

DNA is passed through the three types of chips, the Warburg starts to dominate at higher and higher frequencies with the double-layer capacitive effects vanishing in the perfect channel (Figure 4). In our flow design, mass transport in the solution is enhanced by convection and R_S is significantly reduced. As such, the RC time is much smaller and the Debye branch is shifted to frequencies much higher than the high-frequency asymptote of the Warburg branch. This decoupling of the two branches due to flow preserves the Warburg
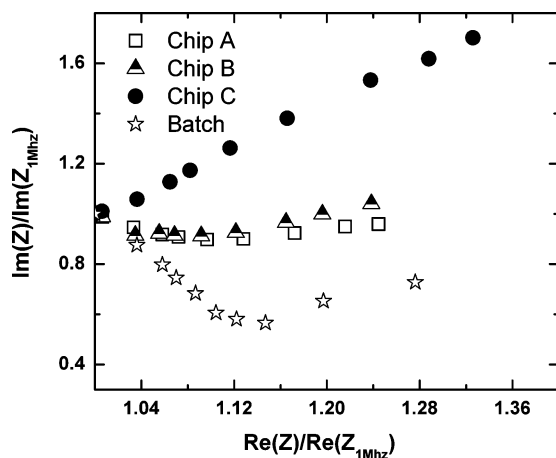
branch to much higher frequencies (Figure 3A), allowing sensitive estimate of R_{Ct}, a measure of the hybridization events that occur near the CNT interface.

Flow is observed to significantly lower R_S (compare Figure 3 to Figure 2) to produce a net resistance $R_f = R_S + R_{Ct}$, representing the intercept of the Warburg branch with the real axis, of no more than 200 Ω. This value is much lower than the kΩ resistance typical of capacitance electrochemical sensing with surface monolayers on the sensing electrodes. After hybridization at 1 MHz in a hybridization buffer, the impedance spectrum is taken during rinsing by a washing PBS buffer at different flow rates. After hybridization, the spectrum at high washing flow rates is observed to shift toward lower values by roughly 50 Ω (Figure 3). This is an appreciable ($>$10%) fraction of the flow-reduced R_f, as is consistent with the expectation that DNA hybridization significantly enhances the electron-transfer rate. It is also larger than the 2 Ω error in our impedance data (see Materials and Methods). This shift can be further amplified with proper data reduction with respect to a control without any DNA molecules. In particular, we seek a resolution that allows us to differentiate between two closely related congeneric species of crustaceans, *Carcinus maenas* and *Carcinus aestuarii*. The targeted gene sequence is a 26 base oligonucleotide fragment of the cytochrome *c* oxidase subunit I mitochondrial gene sequence that is the complementary sequence to the *Carcinus maenas* oligonucleotide sequence.[28] As a stringent test of the specificity of our device, we test our platform with the congeneric species *Carcinus aes-*

Figure 4. Nyquist plots for the unsealed (chip A), partially sealed (chip B), and perfect chips (chip C). To give a good representative picture, the real and imaginary parts have been divided by the corresponding real and imaginary impedance values at 1 MHz. For a qualitative feel of the shift in Warburg, the batch hybridization data from Figure 2 (post hybridization), normalized as above, are also shown.

tuarii that differs from our targeted sequence by three base mismatches at positions 12, 21, and 22 of the 26 base tag sequences (reading from 5′ to 3′, respectively). By fluorescent labeling both the target and the congener DNA and with the same oligo probe functionalized onto silica beads, we have recently shown in an open-flow study that hybridization occurs for the target DNA and not the congener DNA under similar concentrations and flow conditions.[29] We shall test the mismatch discrimination features of the current label-free CNT impedance assay against this earlier study.

To amplify any significant difference due to hybridization, we define a factor χ, which blows up the shift of the Warburg element with changing R_{Ct} by filtering out the contributions from the bulk resistance. It can be observed from the impedance spectra (Figure 5A) that, with increase in frequency, the imaginary portion of the impedance signifying charge accumulation capacitance vanishes as expected and the real part approaches a constant asymptote (Figure 5B), which we label as R_f, the point of intersection of the Warburg with the real axis. R_f is the sum of the charge-transfer resistance R_{Ct} that decreases with target DNA oligo-CNT interaction and a bulk solution resistance R_S that remains the same across all systems provided there is no interference from the double-layer branch. Thus, we define $\chi = \mathrm{Im}(Z)/(\mathrm{Re}(Z) - R_{fC})$, where Z is the impedance and R_{fC} is the R_f for the control with the same sample solution but without the DNA molecules. This control measurement is made prior to passing the actual sample and after 10 min of continuous flow. Two separate impedance spectra measurements at 5 and 10 min yield less than 1% difference in R_{fC}. The index χ blows up toward higher frequency for nontarget DNA (Figure 5C) as both the numerator and denominator go to zero as the charge-transfer resistance does not change. However, in the case of target DNA, the real part R_f is different from R_{fC} and hence χ remains finite at high frequencies. As can be seen in Figure 5C, the small difference in Figure 3A and the 10% difference in Figure 5B are now converted to a 10-fold difference in the value of χ for the target and congener DNA.

To understand the optimum time required for hybridization, under flow and AC electric field, a separate experiment is carried out in a small reservoir with two parallel electrodes separated by 10 μm and is schematically shown as the inset in Figure 6. The buffer solution with oligo-functionalized CNT without any target DNA is considered as the control. It can be observed that hybridization is very fast for 100 nM concentration of both target and congener DNA (Figure 6). The hybridization is rapid and takes about 6 min to observe any change of impedance. The rapid hybridization may be due to field focusing. The induced polarization of the CNT, which acts as a dipole, generates a point of field maxima near the tip of the CNT surface. This secondary high-field gradient drives the DNA dipole[30] be-
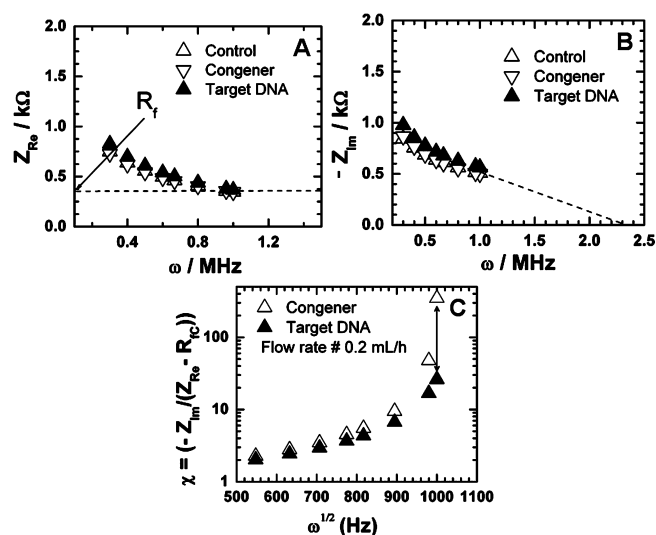

Figure 5. Plots of change in (A) real and (B) imaginary parts of the impedance response. The plot of the modified factor χ with frequency is shown in (C) for the values in (A) and (B).

cause of a large dielectrophoretic force toward the CNT surface, causing rapid hybridization. We believe that this high field gradient may also stretch the long ~500 bases of DNA in the ssPCR sequence to enhance hybridization.[31] If the ssDNA probe absorbs onto the CNT, the high-frequency field may also erect it to expedite hybridization. This enhanced hybridization effect needs to be studied in more detail, and fluorescent correlation spectroscopy (FCS) studies are underway to determine the frequency and the field effects of such dipole−dipole interaction.

To demonstrate the specificity of the flow-based CNT trapped in the microfluidic platform for genetic identification, the following experiment is conducted. A comparative test between green crab and a closely related three-base mismatched congeneric species (*Carcinus aestuarii*) is performed. It is achieved by passing, first, the congener DNA followed by washing with PBS buffer with varying flow rate of 0.01 to 0.2 mL/h,
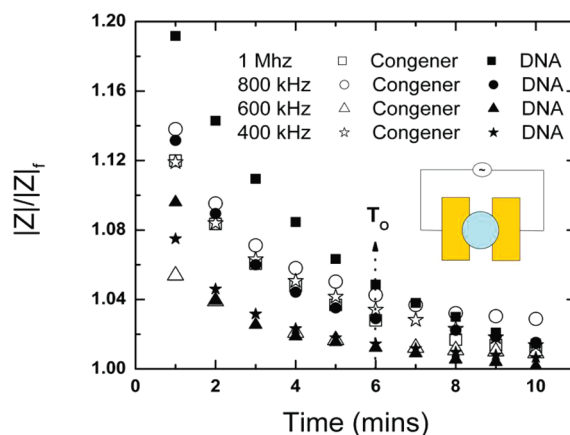

Figure 6. Schematic representation of the process to study the kinetics of DNA hybridization is shown in the inset. The impedance modulus is tracked as a function of time. For visualization purposes, the modulus is plotted with reference to its final value $|Z|_f$ after 15 min to allow for complete saturation.
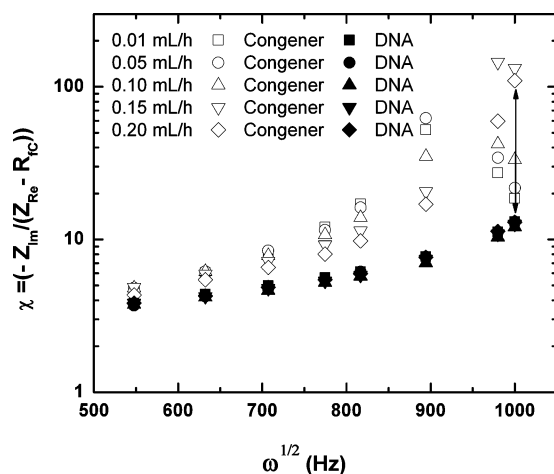
Figure 7. Change in χ with different flow rates ranging from 0.01 to 0.2 mL/h for both target and congener DNA.

and then the green crab DNA is passed through the same chip packed with probe-functionalized (green crab specific) CNT. The measure of hybridization response, χ, separates out considerably for target and congener DNA as the washing buffer flow rate increases from 0.01 to 0.2 mL/h (Figure 7). It can also be seen that at low flow rate the discrimination between target and congener DNA is not possible even at low frequencies. Thus, for the high specificity of the detection platform, the flow rate and the frequency must exceed certain threshold values. We are able to sustain such mismatch discrimination down to picomolar concentrations of target DNA.

The cause of discrimination of the three-base mismatched congener DNA in an open-flow CNT platform is still not clear, and there may be two mechanisms. First, the mechanistic pathway could involve the selective (partial or complete) detachment of nonspecifically attached congener DNA from the CNT surface due to large hydrodynamic shear force. Second, pairing with mismatches may produce much lower electron-transfer rate in the presence of hydrodynamic shear. Careful inspection of Figure 3A, recorded at a high flow rate of 0.2 mL/h, reveals that the Warburg line of the congener DNA (dashed line) approaches two distinct asymptotic values at high and low frequencies. At low frequency, it matches the green crab DNA (Figure 3B), while at high frequency, it shifts toward control, which is functionalized CNT without hybridized DNA (Figure 3C). As the congener impedance always approaches the target impedance and not the control at low frequencies/flow rates, independent of the frequency/flow scan directions, we expect the congener is not completely sheared off the CNT. Just as a high-frequency AC field can possibly enhance the hybridization rate by changing the conformation of the target DNA (Figure 4), it can also affect the conformation of the hybridized DNA and change the electron-transfer rate. At low frequency, the polyvalent counterions, present in the buffer solu-

tion, have sufficient time to migrate toward the electrode, which stabilizes the weakly attached nontarget DNA and may help to transform them into a coiled conformation *via* a condensation mechanism.[32,33] The coiled conformation screens (reduces) the hydrodynamic stress of the flow such that it cannot remove nonspecifically bound molecules. However, at high frequency, near the charge relaxation times of the ions, the polyvalent ions cannot migrate toward the electrode, and DNA remains in the stretched conformation.[34] This stretched conformation is more susceptible to shear flow from the CNT−oligo interface. The conformation of the DNA in the presence of shear and high-frequency AC field is expected to be sensitive to the number and location of mismatches. As a result, the congener DNA may not attach to the CNT as much as the target DNA. Alternatively, the more highly stretched congener DNAs may also block the reacting ions driving the electron-transfer reactions. Finally, these effects of the flow and AC field on the conformation of the hybridized DNA can obviously change the contact between individual CNTs and between CNTs and the electrodes to affect the impedance change. These possible mechanisms await a more detailed molecular-level scrutiny in our subsequent works.

CONCLUSIONS

In this paper, we have successfully demonstrated an open-flow-based rapid, simple, portable, inexpensive, specific, and label-free genetic identification detection technique on a microfluidic platform using CNTs as biosensors. Previous reports on CNT electrode processes in electrochemical batch system demands the employment of different polyvalent ions to magnify the signal output to monitor any significant changes due to docking of DNA as the charge-transfer events are swamped by the formation of the capacitive double layer near the electrode surface. In this present report, we demonstrate a CNT-based microfluidic detection platform with continuous flow that minimizes double-layer formation near CNT interface and thus permit an easy pick up of the impedance signature for the molecular events occurring during DNA docking on the CNT surface. The shear discrimination at high flow and high frequency offers high specificity and allows differentiation between three-base mismatched congener from target DNA sequence. The open-flow design allows the buildup of a large concentration of target biomolecules in the trapped CNT in the microfluidic channel through passage of large volume of low target biomolecules. This leads to enhanced detection sensitivity down to picomolar. We could go further down in detection sensitivity by doping the platform with redox polyvalent ions that promote electron-transfer rate through guanine oxidation,[15] thus extending the detection window to DNA concentrations below picomolar. The development of rapid and portable DNA detection plat-

form will find many important applications in molecular diagnosis, immunoassay-based pathogen detection, trace redox chemical detection, point-of-need and field-use applications, such as epidemic control at ports/airports, avian flu monitoring of poultry imports, environmental monitoring, *etc*.

MATERIALS AND METHODS

Microelectrode Fabrication. The DNA hybridization is performed by trapping the probe-functionalized carbon nanotube (CNT) within a microchannel that is placed between two interdigitated electrodes. These electrodes are fabricated by patterning dual titanium–gold layers onto precleaned 25 × 75 mm glass slides. The slides are patterned with image reversal photoresist Shipley 1813 to generate the electrode patterns by standard photolithography techniques, after which 54 Å of titanium and 261 Å of gold were evaporated onto the slides. This is followed by a resist dissolution and metal liftoff in acetone. The arrays are designed as a parallel assembly of electrodes with a length of 100 μm and width of 10 μm with a pitch of 10 μm.

Microchannel Fabrication. Each slide of patterned microelectrode is cleaned thoroughly by acetone and isopropanol for microchannel fabrication. A photosensitive epoxy-based photoresist, SU 8-25, is spin-coated on one slide. Standard lithography techniques are used for patterning, and the final channel is developed with a SU-8 developer. The dimensions of the SU-8 channel are 25 μm × 100 μm × 100 mm in height × width × length, respectively. The inlet and outlet holes are drilled by a diamond drill onto a second electrode patterned slide.

UV-curable adhesive glue LOCTITE 3492 with a viscosity of 500 Cp is spin-coated onto the slide having the SU-8 layer leaving a 3–5 μm thick coating of glue. When the glue is spin-coated on the chip, it does not enter the channel because of the surface tension of the glue. The two-electrode slides are then aligned by a microscope such that the each spike of parallel array electrodes lies between the two spikes of other slides to form an interdigitated assembly and finally pressed together and exposed to UV to cure the bonding of the two slides together. After applying pressure, the adhesive layer was found to be less than 1 μm thick. To prevent the glue from entering the channel when pressure was applied to the two slides, a small groove was patterned on the outer edges of the desired channel to ensure none of the glue entered the channel. The common method used to bond slides with UV glue is to inject the glue into the chip edge and rely on capillary action to spread the glue. However, the channel is often contaminated by this method. By spinning the glue on the chip and fabricating a groove, contamination of the channel is prevented, allowing for a fast and clean bonding method. To understand the effect of flow on the development of double layer near the electrode, an almost unsealed and partially sealed chip is fabricated. The mostly unsealed chip is fabricated similar to normal chip except the last step where the UV glue is injected into the chip edge and allows the glue to move forward just before the entry point to groove by capillary action so that the liquid only flows through an area surrounding the channel but does not flow through the trapped CNT channel, which is possible due to high pressure gradient in the trapped CNT region. Similarly, the partially sealed chip is fabricated by binding half of the channel properly.

Functionalization of Probe on MWNT Surface. A species-specific amine-functionalized oligonucleotide primer (27mer), complementary to the target green crab DNA, is attach to carboxylated multiwall carbon nanotube (MWNT) by coupling with water-soluble 1-ethyl-3-(3-dimethylaminopropyl)carbodiimide (EDC) and *N*-hydroxysuccinimide (NHS) to produce amide linkages between MWNT and oligomer primer and is performed as reported in literature.[35]

Asymmetric PCR Amplification. To make the CNT-based hybridization platform simpler and also to avoid the denaturation of the target DNA during the hybridization step in the detection platform (*i.e.*, to prevent the denatured dsDNA from recombining before it reaches and interacts with probe-functionalized CNT within the microchannel), asymmetric PCR is executed to produce ssDNA. In this approach, an unequal concentration of primers is used; otherwise, it is analogous to normal, symmetric PCR that produces dsPCR product. In the beginning, amplification starts exponentially, but as the lower concentrated primer gets consumed, the higher concentrated primer continues to amplify only one strand of DNA, thus producing ssDNA. An asymmetric PCR reaction amplifying cytochrome *c* oxidase subunit I (COI) was performed using a forward (0.4 mM concentration) and a reverse primer (0.8 nM concentration) to amplify ~500 bp green crab ssDNA to study on chip DNA hybridization. Similarly, the congeneric primer with three-base mismatches to that of target DNA sequence was amplified for use as a negative control.

Procedure for Flow-Based CNT Hybridization Assay. Figure 1 is the schematic presentation of flow-based CNT hybridization platform. The first step is to pass the probe-functionalized CNT in the microchannel for vertical alignment of CNT in the trapping zone under an AC electric field (Figure 1). The solution is then flown through the channel to completely fill it with the CNT, and afterward, the electric field is applied for alignment. The chip is then saturated with PBS buffer, and impedance is measured, which corresponds to the background level impedance of the functionalized CNT. After successful trapping of CNTs, 20 μL of 1 nM congener ssPCR product suspended in 80 μL 4× SSC hybridization buffer is passed through the chip at 55 °C at a slow flow rate of 0.2 mL/h and with an applied field of 1 MHz and 1 V across the microelectrode array. The flow rate is arrived at from careful observations of saturation times of batch hybridization studies as documented in the Results and Discussion. In the washing step, PBS buffer is passed to get rid of any nonspecific binding of DNA molecules to the surface of the CNT, which is critical for obtaining reliable results. The flow rates for both the background and the washing step are 0.2 mL/h to obtain similar impedance conditions before and after hybridization unless otherwise noted. The change in impedance of the CNT-trapped chips is then measured before and after passing of congener ssPCR product at an AC voltage of 1 V. In the next step, target species (green crab) ssPCR product is passed through the chip under the same conditions and finally washed with PBS to wash off any nonspecific attachment of DNA molecules. Repeated impedance measurements indicate the impedance values to be within 2 Ω, which is much smaller than the 50 Ω shift after hybridization.

REFERENCES AND NOTES

1. Hutvagner, G.; Mclachlan, J.; Pasquinelli, A. E.; Balint, E.; Tuschl, T.; Zamore, P. D. A Cellular Function for the RNA-Interference Enzyme Dicer in the Maturation of the *let-7* Small Temporal RNA. *Science* **2001**, *293*, 834–838.
2. Palecek, E. Surface-Attached Molecular Beacons Light the Way for DNA Sequencing. *Trends Biotechnol.* **2004**, *22*, 55–58.
3. Tu, I.-P.; Schaner, M.; Diehn, M.; Sikic, B. I.; Brown, P. O.; Botstein, D.; Fero, M. J. A Method for Detecting and Correcting Feature Misidentification on Expression Microarrays. *BMC Genomics* **2004**, *5*, 64.
4. Tüdos, A. J.; Besselink, G. A. J.; Schasfoort, R. B. M. Trends in Miniaturized Total Analysis Systems for Point-Of-Care Testing in Clinical Chemistry. *Lab Chip* **2001**, *1*, 83–95.
5. Kian-Kok Ng, J.; Feng, H.; Liu, W. T. Rapid Discrimination of Single-Nucleotide Mismatches Using a Microfluidic Device with Monolayered Beads. *Anal. Chim. Acta* **2007**, *582*, 295–303.

6. Chang, H.-C. Nanobead Electrokinetics: The Enabling Microfluidic Platform for Rapid Multi-Target Pathogen Detection. *AIChE J.* **2007**, *53*, 2486–2492.

7. Sengupta, S.; Battigelli, D. A.; Chang, H.-C. A Micro-Scale Multi-Frequency Reactance Measurement Technique to Detect Bacterial Growth at Low Bio-Particle Concentrations. *Lap Chip* **2006**, *6*, 682–692.

8. Balassubramanian, K.; Burghard, M. Biosensors Based on Carbon Nanotubes. *Anal. Bioanal. Chem.* **2006**, *385*, 452–568.

9. Kelley, S. O.; Holmlin, R. E.; Stemp, E. D. A.; Barton, J. K. Photoinduced Electron Transfer in Ethidium-Modified DNA Duplexes: Dependence on Distance and Base Stacking. *J. Am. Chem. Soc.* **1997**, *119*, 9861–9870.

10. Guo, X.; Gorodetsky, A. A.; Hone, J.; Barton, J. K.; Nuckolls, C. Conductivity of a Single DNA Duplex Bridging a Carbon Nanotube Gap. *Nat. Nanotechnol.* **2008**, *3*, 163–167.

11. Degefa, T. H.; Kwak, J. Electrochemical Impedance Sensing of DNA at PNA Self Assembled Monolayer. *J. Electroanal. Chem.* **2008**, *612*, 37–41.

12. Kuhr, W. G. Electrochemical DNA Analysis Comes of Age. *Nat. Biotechnol.* **2000**, *18*, 1042–1043.

13. Sosnowski, R. G.; Tu, E.; Butler, W. F.; O'Connell, J. P.; Heller, M. J. Rapid Determination of Single Base Mismatch Mutations in DNA Hybrids by Direct Electric Field Control. *Proc. Natl. Acad. Sci. U.S.A.* **1997**, *94*, 1119–1123.

14. Zhou, R.; Wang, P.; Chang, H.-C. Bacteria Capture, Concentration and Detection by Alternating Current Dielectrophoresis and Self-Assembly of Dispersed Single-Wall Carbon Nanotubes. *Electrophoresis* **2006**, *27*, 1376–1385.

15. Li, J.; Hou, T. N.; Cassell, A.; Fan, W.; Chen, H.; Ye, Q.; Koehne, J.; Han, J.; Meyyappan, M. Carbon Nanotube Nanoelectrode Array for Ultrasensitive DNA Detection. *Nano Lett.* **2003**, *3*, 597–602.

16. Maehashi, K.; Matsumoto, K.; Kerman, K.; Takamura, Y.; Tamiya, E. Ultrasensitive Detection of DNA Hybridization Using Carbon Nanotube Field-Effect Transistors. *Jpn. J. Appl. Phys.* **2004**, *43*, L1558–L1560.

17. Xu, Y.; Ye, X.; Yang, L.; He, P.; Fang, Y. Impedance DNA Biosensor Using Electropolymerized Polypyrrole/Multiwalled Carbon Nanotubes Modified Electrode. *Electroanalysis* **2006**, *18*, 1471–1478.

18. Dawson, J. L.; John, D. G. Diffusion Impedance—An Extended General Analysis. *J. Electroanal. Chem.* **1980**, *10*, 37–47.

19. Sambrook, J.; Fritsch, E. F.; Maniatis, T. *Molecule Cloning: A Laboratory Manual*; 2nd ed.; Cold Spring Harbor: New York, 1989.

20. Varma, R.; Selman, J. R. *Techniques for Characterization of Electrodes and Electrochemical Processes*; Wiley: New York, 1991.

21. Bard, A. J.; Faulkne, L. R. *Electrochemical Methods: Fundamentals and Applications*; Wiley: New York, 1980.

22. Mauracher, P.; Karden, E. Dynamic Modelling of Lead/Acid Batteries Using Impedance Spectroscopy for Parameter Identification. *J. Power Sources* **1997**, *67*, 69–84.

23. Taylor, S. R.; Gileadi, E. Physical Interpretation of the Warburg Impedance. *Corrosion* **1995**, *51*, 664–671.

24. Muralidharan, V. S. Warburg Impedance-Basics Revisited. *Anti-Corros. Methods Mater.* **1997**, *44*, 26–29.

25. Cai, H.; Cao, X.; Jiang, Y.; He, P.; Fang, Y. Carbon Nanotube-Enhanced Electrochemical DNA Biosensor for DNA Hybridization Detection. *Anal. Bioanal. Chem.* **2003**, *375*, 287–293.

26. Bardea, A.; Katz, E.; Willner, I. Probing Antigen−Antibody Interactions on Electrode Supports by the Biocatalyzed Precipitation of an Insoluble Product. *Electroanalysis* **2000**, *12*, 1097–1106.

27. Xu, Y.; Jiang, Y.; Cai, H.; He, P.-G.; Fang, Y.-Z. Electrochemical Impedance Detection of DNA Hybridization Based on the Formation of M-DNA on Polypyrrole/Carbon Nanotube Modified Electrode. *Anal. Chim. Acta* **2004**, *516*, 19–27.

28. Mahon, A. R. Unpublished data.

29. Senapati, S.; Mahon, A. R.; Gordon, J.; Nowak, C.; Sengupta, S.; Powell, T. H. W.; Feder, J.; Lodge, D. M.; Chang, H.-C. Rapid On-Chip Genetic Detection Microfluidic Platform for Real World Applications. *Biomicrofluidics* **2009**, *3*, 022407-7.

30. Kim, D. R.; Zheng, X. Numerical Characterization and Optimization of the Microfluidics for Nanowire Biosensors. *Nano Lett.* **2008**, *8*, 3233–3237.

31. Asbury, C. L.; Engh, G. V. D. Trapping of DNA in Nonuniform Oscillating Electric Fields. *Biophys. J.* **1998**, *74*, 1024–1030.

32. Asbury, C. L.; Diercks, A. H.; Engh, G. V. D. Trapping of DNA by Dielectrophoresis. *Electrophoresis* **2002**, *23*, 2658–2666.

33. Gagnon, Z.; Senapati, S.; Gordon, J.; Chang, H.-C. Dielectrophoretic Detection and Quantification of Hybridized DNA Molecules on Nano-Genetic Particles. *Electrophoresis* **2008**, *29*, 4808–4812.

34. Rouzina, I.; Bloomfield, V. A. DNA Bending by Small, Mobile Multivalent Cations. *Biophys. J.* **1998**, *74*, 3152–3164.

35. Marquette, C. A.; Blum, L. J. Beads Arraying and Beads Used in DNA Chips. *Top. Curr. Chem.* **2006**, *261*, 113–129.